THERMAL BOUNDARY LAYER IN A CYLINDRICAL GAS COLUMN CONTAINING BULK SOURCES AND A BIFILAR CURRENT

S. V. Nikonov and Yu. V. Sanochkin

UDC 533.6.011

Parameters have been calculated [1] for the thermal layer arising on longitudinal flow of an unbounded cylindrical column of gas with an arbitrary distribution of the sources.

Here we consider the thermal boundary layer for the more complicated case where there is a distributed bifilar current along with the cylindrical region of heat input. The current in one direction flows through the volume where the heat is produced, while the reverse current, which is equal in magnitude, flows in the current layer (part of the thermal layer) in accordance with the distribution of the gas conductivity. The magnetic field vanishes outside the current layer, while within it the interaction between the currents and the induced magnetic field results in ponderomotive forces. A difference from [1] is that the flow in that case is not in general isobaric. The current produces Joule heating, namely an additional bulk heat source, which extends to the entire current layer and which may play an important part in the energy balance. We consider the stationary state on the assumption that thermal conduction is the main mode of heat loss. The problem can be formulated as follows in a frame of reference coupled to the free flow: One has to determine the structures of the thermal and current boundary layers formed in rectilinear motion of distributed heat sources and the bifilar current in the gas.

1. Figure 1 shows the disposition of the axes of the cylindrical coordinate system and the sections of the thermal and current layers. The forward current I with density $\mathbf{j}_0 = (0, 0, j_0)$ is localized in a column of radius a and sets up the azimuthal magnetic field $\mathbf{B}_0 = (0, B_0, 0)$. The reverse current with density $\mathbf{j} = (j_r, 0, -j_z)$ produces the opposite field $\mathbf{B}' = (0, -B', 0)$. The component j_r of the reverse current is localized in the main in a small region of the initial section. The total magnetic field $\mathbf{B} = (0, B, 0)$ can be written as

$$B = B_0 - B' = \mu/2\pi r(J_0 - J),$$

where

$$J_0 = \int_0^r 2\pi r j_0 dr, \; J = \int_0^r 2\pi r j_z dr, \tag{1.1}$$

and μ is the magnetic permeability. The output of the external heat sources is

$$q = b\rho, \quad b = \begin{cases} b = \text{const}, & (r \leqslant a), \\ 0, & (r > a). \end{cases}$$

The discussion below can be transferred directly to the case of any $q(\rho, h)$ relation. The law adopted for the energy production applies in particular when a flux of charged particles is retarded by ionization in matter [2]. The electric field provides for the passage of the reverse current. It is assumed that the current distribution can be described by a scalar conductivity

$$\mathbf{j} = \sigma(\mathbf{E} + \mathbf{v}\times\mathbf{B}), \tag{1.2}$$

where $\mathbf{v} = (v, 0, u)$ is the gas speed. The following is the initial system of equations for a perfect nonviscous gas in the absence of flow spiralling

$$\partial(r\rho v)/\partial r + \partial(r\rho u)/\partial z = 0; \tag{1.3}$$

$$\rho(v\,\partial u/\partial r + u\,\partial u/\partial z) = -\partial p/\partial z + j_r B; \tag{1.4}$$

$$\rho(v\,\partial v/\partial r + u\,\partial v/\partial z) = -\partial p/\partial r + j_z B; \tag{1.5}$$

$$\rho(v\,\partial h/\partial r + u\,\partial h/\partial z) = v\,\partial p/\partial r + u\partial p/\partial z + \mathrm{div}((\lambda/c_p)\nabla h) + q + j^2/\sigma; \tag{1.6}$$

$$p = ((\gamma - 1)/\gamma)\rho h. \tag{1.7}$$

Moscow. Translated from Zhurnal Prikladnoi Mekhaniki i Tekhnicheskoi Fiziki, No. 5, pp. 78-84, September-October, 1982. Original article submitted July 16, 1981.

 0021-8944/82/2305-0662$07.50

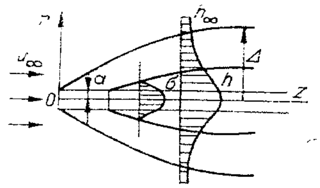

Fig. 1

Here p is pressure, h specific enthalpy, λ thermal conductivity, c_p specific heat, and γ the adiabatic parameter. In (1.4) and (1.5) we have omitted the $j_0 \times B$ term, and in the energy equation we have incorporated only the ohmic dissipation for the reverse current. These assumptions are correct for example when the forward current is transported by a flux of relativistic electrons.

2. The system (1.2)-(1.7) can be simplified substantially for this model. As j_r is small everywhere apart from near the origin, there can be marked changes in the axial velocity and pressure along z only within this region. We assume further that the pressure is only slightly dependent on z within the thermal layer (calculations for the entire range of conditions confirm this, as the pressure hardly varies along the axis of the thermal layer). Then (1.4) shows that we can neglect the change in the axial velocity of the flow to a first approximation and put

$$u \simeq \text{const.} \tag{2.1}$$

The integral of (2.1) is exact in the absence of ponderomotive forces and is given in [3] for an electric arc. In [3, 4] we find bounds for the increment in the longitudinal velocity and the variation with z. We can certainly neglect the change in the axial velocity if $\mu I^2/(8\pi^2\rho_\infty u_\infty^2 a^2) \ll 1$, but in practice the region is much wider. It is also permissible to put $u \simeq u_\infty$, since the effects of the error arising at the start of the layer vanish as z increases.

Equation (1.5) in the boundary-layer approximation is a condition for radial equilibria $\partial p/\partial r = j_z B$, or in integral form

$$p = p_\infty - \frac{\mu}{2\pi}\int_r^\infty \frac{dr}{r}\, j_z (J_0 - J). \tag{2.2}$$

We eliminate the electric field from (1.2) and integrate the resulting equation with respect to r within the thermal layer to get

$$E_z|_{r=\Delta} - E_z|_{r=0} = -u_\infty \frac{d}{dz}\int_0^\Delta B dr \sim \frac{\Delta}{l}. \tag{2.3}$$

As v is small, one can neglect the induced current in (1.2) for j_z and write Ohm's law as

$$j_z = \sigma E_z \tag{2.4}$$

or an integral form on the basis that the current is bidirectional

$$I = E_z \int_0^\Delta 2\pi r \sigma dr. \tag{2.5}$$

The following is the energy equation (1.6) in the boundary-layer approximation:

$$\rho v \frac{\partial h}{\partial r} + \rho u \frac{\partial h}{\partial z} = v \frac{\partial p}{\partial r} + u \frac{\partial p}{\partial z} + \frac{1}{r}\frac{\partial}{\partial r}\left(r \frac{\lambda}{c_p}\frac{\partial h}{\partial r}\right) + q + j_z E_z. \tag{2.6}$$

The boundary conditions are

$$v|_{r>0} = 0,\ h|_{z=0} = h_\infty,\ h|_{r\to\infty} = h_\infty,\ \partial h/\partial r|_{r=0} = 0,\ v|_{z=0} = 0,$$
$$dh/\partial r|_{r\to\infty} = 0,\ \partial\rho/\partial r|_{r=0} = 0,\ \rho|_{z=0} = \rho_\infty,\ \rho|_{r\to\infty} = \rho_\infty.$$

3. We follow [3, 4] and solve the problem by an approximate method similar to the Karman–Polhausen integral method. We integrate (1.3) and (2.6) with respect to r within the thermal layer and eliminate $v(\Delta, z)$ to get

$$\frac{d}{dz}\Delta_h^2 = Q_p + \frac{IE_z}{\pi u_\infty \rho_\infty h_\infty} + \frac{ba^2\rho_m}{\rho_\infty h_\infty u_\infty}, \tag{3.1}$$

where

$$Q_p = \frac{2}{u_\infty \rho_\infty h_\infty} \int_0^\Delta r\left(v \frac{\partial p}{\partial r} + u_\infty \frac{\partial p}{\partial z}\right) dr;$$

$$\Delta_h^2 = 2\int_0^\Delta \frac{\rho}{\rho_\infty}\left(\frac{h}{h_\infty} - 1\right) r dr = 2\Delta^2 \int_0^1 \frac{\rho}{\rho_\infty}\left(\frac{h}{h_\infty} - 1\right)\eta d\eta = k\left(\frac{h_m}{h_\infty} - 1\right)\frac{\rho_m}{\rho_\infty}\Delta^2. \tag{3.2}$$

Here Δ_h is the thickness of the layer in which enthalpy is acquired, while Q_p is the heat source associated with pressure change, $\eta = r/\Delta$, and the subscript m indicates values of variables at the axis. The heat arising because of friction and compression on flow over a solid impermeable surface is important if the flow speed is so high that the rise in temperature from adiabatic compression is of the order of the temperature difference between the body and the gas at infinity [5]. In the present case of a permeable obstacle, the compression effect is naturally much less (for example, there is no pressure change at all if electromagnetic effects are absent [1]. Also, as z increases the temperature difference within the thermal layer considerably exceeds the temperature level in the free flow. Therefore, Q_p will be neglected in what follows. In that case a solution can be obtained by using a one-parameter approximation for the enthalpy profile:

$$h = h_\infty + (h_m - h_\infty)f(\eta),$$

where the function $f(\eta)$ satisfies the conditions

$$f(0) = 1,\ f'(0) = 0,\ f(1) = 0,\ f'(1) = 0,\ f''(1) = 0, \ldots \tag{3.3}$$

The conditions of (3.3) are satisfied by the polynomial

$$f(\eta) = (1 - \eta)^N(1 + N\eta).$$

We used a polynomial of fourth degree (N=3). The coefficient k in (3.2) is a function of ρ_m:

$$k = \int_0^1 2\frac{\rho}{\rho_m} f(\eta)\,\eta d\eta \geqslant k_1 = \int_0^1 2f(\eta)\,\eta d\eta. \tag{3.4}$$

According to (3.4), $k_1 = 0.2$ for N=3; if there is a greater reduction, when the mean density $\bar{\rho} \gg \rho_m$, then we have $k < 1$. One can take k as approximately constant ($k \lessdot 1$) because the effects of the inaccuracy permitted in the initial part vanish as we move away from the start of the layer.

Equations (2.6) and (2.2) take the following form at the axis:

$$\rho_m u_\infty \frac{dh_m}{dz} = b\rho_m + \sigma_m E_z^2 - \frac{2N(N+1)}{\Delta^2}\frac{\lambda_m}{c_{pm}}(h_m - h_\infty); \tag{3.5}$$

$$p_m = p_\infty - \frac{\mu E_z}{2\pi}\int_0^\Delta \frac{dr}{r}\sigma(J_0 - J). \tag{3.6}$$

The system (1.7), (2.5), (3.1), (3.5), (3.6) enables one to determine Δ_h, h_m, ρ_m, p_m, E_z; we use the following approximations for the properties of the medium [4]:

$$\frac{\lambda_m}{c_{pm}} = \frac{\lambda_\infty}{c_{p\infty}}\sqrt{\frac{h_m}{h_\infty}},\quad \sigma(h) = \sigma_0\sqrt{\frac{h}{h_\infty}}\exp\left(-\frac{\alpha h_\infty}{h}\right). \tag{3.7}$$

Formula (3.7) for the conductivity describes the transition from a cold gas to a weakly ionized one satisfactorily. We have $\sigma_0 = 430$ mho/m, $\alpha = 187$ for air under normal conditions. It is convenient to isolate the radial dependence of σ in explicit form:

$$\sigma = \sigma_m(h_m)\sigma'(z, \eta),\ \sigma' \leqslant 1,$$

where $\sigma' = \sqrt{f + \frac{h_\infty}{h_m}(1 - f)}\exp\left\{-\frac{\alpha h_\infty}{h_m}\frac{(h_m - h_\infty)(1 - f)}{h_\infty + (h_m - h_\infty)f}\right\}.$

We put $\omega(\eta) = \int_0^\eta \eta\sigma' d\eta$, $\omega_1 = \omega(1)$, to write (1.1) and (2.5) as

$$J = 2\pi\omega\sigma_m E_z\Delta^2,\ I = 2\pi\omega_1\sigma_m E_z\Delta^2 \tag{3.8}$$

correspondingly. Assuming for definiteness that j_0 = constant we get from (1.1) that

$$J_0 = Ii_0(\eta), \tag{3.9}$$

where $i_0(\eta) = \begin{cases}(\Delta^2/a^2)\,\eta^2, & (\eta < a/\Delta),\\ 1, & (\eta \geqslant a/\Delta).\end{cases}$

We introduce the dimensionless variables

$$x = bz/h_\infty u_\infty,\quad \psi = \Delta_h^2/a^2,\quad g = h_m/h_\infty,\quad \bar{p} = p_m/p_\infty,$$
$$\bar{\rho} = \rho_m/\rho_\infty,\quad \bar{\sigma} = \sigma_m/\sigma_0,\quad \varepsilon = 4\pi a^2\sigma_0 E_z/kI$$

(the bars are subsequently omitted). The system becomes

$$d\psi/dx = \rho + G\varepsilon; \tag{3.10}$$

$$dg/dx = 1 + (k/4)G\sigma\varepsilon^2/\rho - \Lambda(g-1)^2\sqrt{g}/\psi; \tag{3.11}$$

$$\varepsilon = 2(g-1)\rho/(\sigma\psi\omega_1); \tag{3.12}$$

$$p = 1 - \mathscr{P}\,\frac{2(g-1)\rho}{\psi\omega_1}\int\limits_0^1 \frac{d\eta}{\eta}\,\sigma'\left(i_0 - \frac{\omega}{\omega_1}\right); \tag{3.13}$$

$$p = \rho g, \tag{3.14}$$

where $G = kI^2/(4\pi^2 a^4\sigma_0 b\rho_\infty)$; $\mathscr{P} = k\mu I^2/(8\pi^2 a^2 p_\infty)$, $\Lambda = 2N(N+1)k\lambda_\infty h_\infty/(a^2 c_{p\infty} b\rho_\infty)$. The problem contains three similarity criteria G, $\mathscr{P}$, Λ instead of Λ along in [1]; G is the ratio of the Joule heating to the heating from the external bulk heat sources, while $\mathscr{P}$ is the ratio of the magnetic pressure to the gas-kinetic value. The boundary conditions are $\psi(0)=0$, $g(0)=1$, $\rho(0)=1$, $p(0)=1$.

4. The characteristic feature of this problem is similar to a feature in the problems of boundary-layer type and lies in the formation of the initial conditions at $x=0$ (singular point). If we assume that the thermal layer has a thickness $\sim a$ at $x=0$, then the solution is incorrect at distances of the order of several a near the initial section because equations of boundary-layer type do not apply in that region. Also, the conditions for smallness of j_r do not apply near the initial section, nor does the bound of (2.3) for the electric field, and therefore expression (2.4) for Ohm's law does not apply, nor do certain approximations such as (3.9). As $\sigma \to 0$ at the start of the layer (Fig. 1) we have for (3.8) that $E_z \to \infty$ if $i=$ constant. To avoid this difficulty in numerical solution we take the current in the initial section as varying in accordance with

$$I(1 - e^{-\varkappa\sigma})\quad (\varkappa > 0).$$

The following relation is typical for this wide range in the parameters: for $\varkappa = 10^3$-10^4 the current is cut in for $x \approx 10$, and for $\varkappa = 10^8$ for $x \approx 4$-5. The solutions are rapidly varying functions of the coordinate near the region of current cut in and naturally vary with $\varkappa$. However, one expects that the effects of the initial zone will become weaker as we move away from the start of the layer and that the solutions for the various approximations near zero will come together. Calculations confirm this. For example, the g(x) curves for various $\varkappa$ differ by 3-5 orders of magnitude, come together as x increases, and differ by only 2-3% for $x \approx 10^2$.

For $\mathscr{P} = G = 0$ Eqs. (3.10)-(3.14) become the system examined in [1]. In particular, a detailed study was made there of the asymptotes of the solutions for $x \to 0$, $x \to \infty$, $\Lambda \to 0$. One can obtain analogous expansions for system (3.10)-(3.14) for the case $\mathscr{P} = 0$; these are very cumbersome and are not given. We merely note that the singularities on the right sides of (3.10)-(3.13) at $x=0$ can be removed. In the general case of arbitrary values of the similarity criteria $\mathscr{P}$, G, Λ the system (3.10)-(3.14) has been integrated numerically, and most of the calculations were performed for $\varkappa = 10^3$-10^4.

5. Figure 2 shows the enthalpy profiles 2 ($1 - \mathscr{P} = 0$, $G = 0$, $\Lambda = 0$; $2 - \mathscr{P} = 0$, $G = 10^{-4}$, $\Lambda = 0$; $3 - \mathscr{P} = 0$, $G = 10^{-2}$, $\Lambda = 0$; $4 - \mathscr{P} = 1$, $G = 10^{-2}$, $\Lambda = 0$; $5 - \mathscr{P} = 1$, $G = 10^{-2}$, $\Lambda = 10^{-3}$; $6 - \mathscr{P} = 0$, $G = 0$, $\Lambda = 10^{-3}$). Curve 1 is described by the formula $g = 1 + x$ and gives the enthalpy distribution in the absence of current and heat transfer. Comparison of curves 1, 2, and 3 indicates that there is a marked effect from ohmic dissipation by the reverse current on the gas heating. Curves 2 and 3 initially rise rapidly because of the current switch in, but the rise becomes slower as x increases and the slope approximates to the slope of curve 1, which means that the role of the Joule heating falls as the channel heats up and the conductivity increases (the difference in the ordinates for curves 2 and 1 for a given x gives the enthalpy due to the current dissipation). There is a relatively small effect from the pressure change in the layer as regards the enthalpy (curves 3 and 4), which agrees with the previous assumption about the neglect of Q_p. The sign of the effect has a clear physical meaning: Pressure reduction leads to gas cooling. Finally, comparison of curves 1 and 6 with 4 and 5 confirms the important role of heat transfer in the correct estimation of the enthalpy at the axis.

Particular interest attaches to the density reduction in the gas within the thermal layer. Figure 3 shows the theoretical results for the density as a function of the coordinate ($1 - \mathscr{P} = 0$, $G = 0$, $\Lambda = 0$; $2 - \mathscr{P} = 0$, $G =$

TABLE 1

$\mathscr{P}$	G	Λ	p_{min}	$\mathscr{P}$	G	Λ	p_{min}
0,1	10^{-2}	0	0,738	1	0	0	0,0478
1	10^{-2}	0	0,102	1	10^{-2}	10^{-3}	0,138

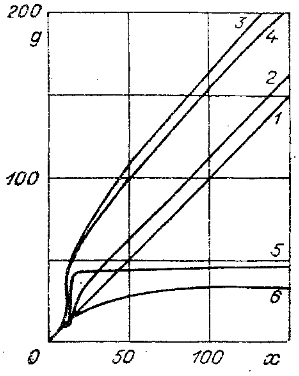

Fig. 2

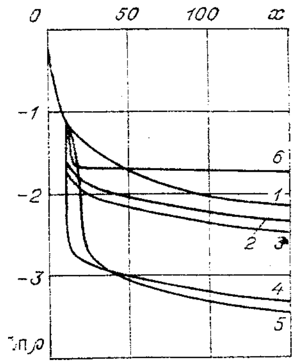

Fig. 3

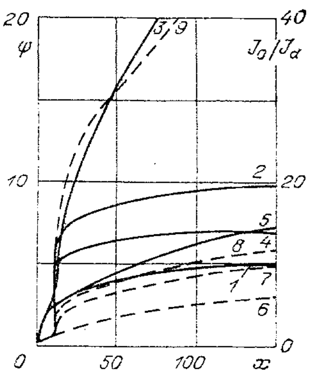

Fig. 4

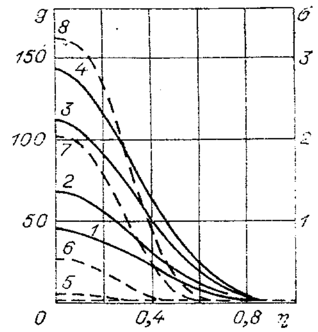

Fig. 5

10^{-2}, $\Lambda = 0$; $3 - \mathscr{P} = 0{,}1$; $G = 10^{-2}$, $\Lambda = 0$; $4 - \mathscr{P} = 1$, $G = 10^{-2}$, $\Lambda = 0$; $5 - \mathscr{P} = 1, G = 0, \Lambda = 0$; $6 - \mathscr{P} = 0, G = 10^{-2}$, $\Lambda = 10^{-3}$) ; curve 1 is described by the equation $\rho = (1 + x)^{-1}$ and gives the density distribution in the absence of current and heat transfer. The Joule heating has a relatively small effect on the density change (curves 1 and 2), whereas the pressure reduction in the boundary layer produces a considerable density change (curves 2 and 3 as against 3 and 4 or 1 and 5). The density reduction may increase by an order or more. As regards the effects of Joule heating and pressure change in the layer we can say that the effect of the first is seen mainly in the enthalpy change, while the second is seen mainly in the density. The heat transfer substantially reduces g and increases the density in the layer, so it should be incorporated.

The solution can be checked from p(x), which takes the following form: The pressure falls to p_{min} then increases very slightly with x when the reverse current attains its maximum value. Table 1 illustrates the dependence of p_{min} on the parameters.

Figure 4 shows the variation of the enthalpy-input layer thickness with the coordinate for various values of the similarity criteria (solid lines $1 - \mathscr{P} = 0$, $G = 0$, $\Lambda = 0$; $2 - \mathscr{P} = 0$, $G = 10^{-2}$, $\Lambda = 0$; $3 - \mathscr{P} = 0$, $G = 10^{-2}$, $\Lambda = 10^{-3}$; $4 - \mathscr{P} = 1$, $G = 10^{-2}$, $\Lambda = 0$; $5 - \mathscr{P} = 0$, $G = 0$, $\Lambda = 10^{-3}$). Curve 1 is described by the formula $\psi = \ln(1 + x)$ and represents the layer in the absence of current and heat transfer. Joule heating produces an appreciable increase in the thickness (curves 1 and 2). Heat transfer also increases the thickness (compare curves 2 and 3 with 1 and 5), and when these two effects go together there is particularly marked expansion of the layer (Fig. 3). Conversely, the pressure change in the layer reduces the thickness (curves 2 and 4).

Broken lines 6-9 in Fig. 4 show the redistribution of the reverse current over the cross section of the current layer as the thickness increases ($6 - \mathscr{P} = 0$, $G = 10^{-4}$, $\Lambda = 0$; $7 - \mathscr{P} = 0$, $G = 10^{-2}$, $\Lambda = 0$; $8 - \mathscr{P} = 0{,}1$, $G = 10^{-2}$, $\Lambda = 0$; $9 - \mathscr{P} = 1$, $G = 10^{-2}$, $\Lambda = 0$) ; the ordinate shows the ratio of the proportion of the reverse current J_0 flowing outside the current tube with radius a to the value of the reverse current J_a flow at $r<a$. The magnetic pressure tends to displace the reverse current from the axis towards the periphery, but the thickness of the current layer and the current distribution in it are determined by the conductivity profile. The graphs show that the proportion of the peripheral current increases monotonically with x. The Joule heating and the pressure reduction in the layer tend to increase J_0/J_a, whereas the value is largely unaffected by the heat transfer.

Finally, Fig. 5 shows typical enthalpy distributions (solid lines 1-4) along with conductivity ones (broken lines 5-8) transverse to the thermal layer for various values of x ($\mathscr{P} = 1$, $G = 10^{-2}$, $\Lambda = 0$, curves 1 and 5 correspond to $x = 13.5$; 2, $6 - x = 24.7$; 3, $7 - x = 61.7$; 4, $8 - x = 87.7$). The thickness of the current layer is about half the thickness of the thermal layer and increases somewhat with x. The graphs illustrate that the increase in the conductivity is rapid by comparison with that in the enthalpy in the initial part and that the profile is drawn out, which is characteristic of weakly ionized plasma.

In conclusion we consider briefly the variations in the electromagnetic quantities. The axial electric field is maximal at the start of the layer and decreases monotonically as x increases. The fall is correlated with the increase in the conductivity and thickness of the thermal layer by the constant-current condition (3.12). The mean values of the magnetic field and the radial electric field decrease in accordance with the increase in current layer thickness. The mean density of the reverse current decreases as x increases more rapidly than the thickness of the current layer increases.

We are indebted to M. A. Vlasov, S. I. Vybornov, and A. V. Zharinov for discussions.

LITERATURE CITED

1. Yu. V. Sanochkin, "The thermal boundary layer on a cylindrical column of gas with distributed heat sources," Zh. Prikl. Mekh. Tekh. Fiz., No. 3 (1982).
2. Yu. M. Shirokov and N. P. Yudin, Nuclear Physics [in Russian], Nauka, Moscow (1972).
3. B. A. Uryukov, "A longitudinally injected electric arc in a cylindrical channel," Izv. Sib. Otd. Akad. Nauk SSSR, Ser. Tekh. Nauk, Issue 1, No. 3 (1968).
4. M. F. Zhukov, A. S. Koroteev, and B. A. Uryukov, Applied Dynamics of Thermal Plasma [in Russian], Nauka, Novosibirsk (1975).
5. H. Schlichting, Boundary Layer Theory, McGraw-Hill.